PLANT SCIENCES

Neurotoxic peptides from the venom of the giant Australian stinging tree

Edward K. Gilding[1]*, Sina Jami[1]*, Jennifer R. Deuis[1]*, Mathilde R. Israel[1,2], Peta J. Harvey[1], Aaron G. Poth[1], Fabian B. H. Rehm[1], Jennifer L. Stow[1], Samuel D. Robinson[1], Kuok Yap[1], Darren L. Brown[1], Brett R. Hamilton[3], David Andersson[2], David J. Craik[1], Irina Vetter[1,4†], Thomas Durek[1†]

Stinging trees from Australasia produce remarkably persistent and painful stings upon contact of their stiff epidermal hairs, called trichomes, with mammalian skin. *Dendrocnide*-induced acute pain typically lasts for several hours, and intermittent painful flares can persist for days and weeks. Pharmacological activity has been attributed to small-molecule neurotransmitters and inflammatory mediators, but these compounds alone cannot explain the observed sensory effects. We show here that the venoms of Australian *Dendrocnide* species contain heretofore unknown pain-inducing peptides that potently activate mouse sensory neurons and delay inactivation of voltage-gated sodium channels. These neurotoxins localize specifically to the stinging hairs and are miniproteins of 4 kDa, whose 3D structure is stabilized in an inhibitory cystine knot motif, a characteristic shared with neurotoxins found in spider and cone snail venoms. Our results provide an intriguing example of inter-kingdom convergent evolution of animal and plant venoms with shared modes of delivery, molecular structure, and pharmacology.

INTRODUCTION

Australia notoriously harbors some of the world's most venomous animals, but although less well known, its venomous flora is equally remarkable. The giant Australian stinging tree *Dendrocnide excelsa* reigns superlative in size, with some specimens growing to 35 m tall along the slopes and gullies of eastern Australian rainforests (fig. S1). However, these members of the *Urticaceae* family are far more than oversized nettles. Of the six *Dendrocnide* species native to the subtropical and tropical forests of Eastern Australia, *D. excelsa* (*lit.* tall stinging tree) and *D. moroides* (*lit.* mulberry-like stinging tree) are particularly notorious for producing excruciatingly painful stings, which—unlike those of their European and North American relatives—can cause symptoms that last for days or weeks in extreme cases (*1*, *2*). In the state of Queensland, it is not uncommon to find warning signs along forest tracks, alerting unwary visitors to the presence of *Dendrocnide* species and the potency of their sting (Fig. 1A). This signage is justified given that *D. moroides* has been implicated in hospitalization of two individuals requiring intensive care for 36 hours who suffered from acute pain that reportedly did not respond to morphine and ongoing symptoms lasting months (*3*). This long-lasting pain is also typical of other *Dendrocnide* species stings, with episodic pain typically subsiding over several weeks, although paresthesiae may persist longer (*4*).

However, although *Dendrocnide* stings are common and many Australians—including the authors—vividly recall their personal experiences with stinging trees, most of the cases do not require hospitalization, and accordingly, there is little literature systematically evaluating the clinical presentation. Generally, severe pain is the predominant symptom, although neuromuscular symptoms and respiratory distress have also been reported (*2*, *3*). In addition to simple or opioid analgesics, the severe pain is anecdotally treated with dilute hydrochloric acid—presumed to denature venom components—or wax strips, based on the likely erroneous assumption that persistent symptoms are caused mechanically through stinging hairs remaining embedded in the skin.

Like other stinging nettles of the Urticaceae family, the leaves and stems of *D. excelsa* and *D. moroides* are covered with needle-shaped trichomes resembling a covering of deceptively benign felt-like hairs (Fig. 1, B and C). These silicified secretory structures act as hypodermic needles (*5*) that, upon contact with skin, inject specific pharmacological mediators contained within the trichome fluid, leading to activation of nerve terminals innervating the skin (*6*, *7*).

Several small-molecule compounds have been proposed to account for the observed physiological effects of common *Urtica* stings. These irritation-inducing molecules include histamine, acetylcholine, 5-hydroxytryptamine (*8*–*10*), as well as formic acid and other low–molecular weight organic acids (*11*). Although these compounds may explain some immediate discomfort associated with nettle stings, intradermal injection of dialyzed stinging hair extract containing none of these small molecules in the volar forearm of humans was entirely sufficient to reproduce the symptoms of a *Dendrocnide* sting, and addition of histamine, acetylcholine, and 5-hydroxytryptamine at amounts measured from trichomes neither changed the nature of the pain caused by *Dendrocnide* extract nor caused substantial long-lasting pain if injected alone (*2*). The inability to replicate the remarkable severity and extended duration of the pain with the small-molecule mixture suggests the presence of unidentified neurotoxins and inspired our investigation into the pharmacological basis of pain induced by the giant Australian stinging tree.

RESULTS

Pain-inducing compounds from *Dendrocnide* venom

The stings are mediated by trichomes that measure up to about 7 mm in length in *D. excelsa* and *D. moroides* (Fig. 1, B and C). It is

[1]Institute for Molecular Bioscience, The University of Queensland, Brisbane, QLD 4072, Australia. [2]Wolfson Centre for Age-Related Diseases, Institute of Psychiatry, Psychology & Neuroscience, King's College London, London SE5 8AF, UK. [3]Centre for Microscopy and Microanalysis, The University of Queensland, Brisbane, QLD 4072, Australia. [4]School of Pharmacy, The University of Queensland, Brisbane, QLD 4102, Australia.
*These authors contributed equally to this work.
†Corresponding author. Email: i.vetter@uq.edu.au (I.V.); t.durek@uq.edu.au (T.D.)

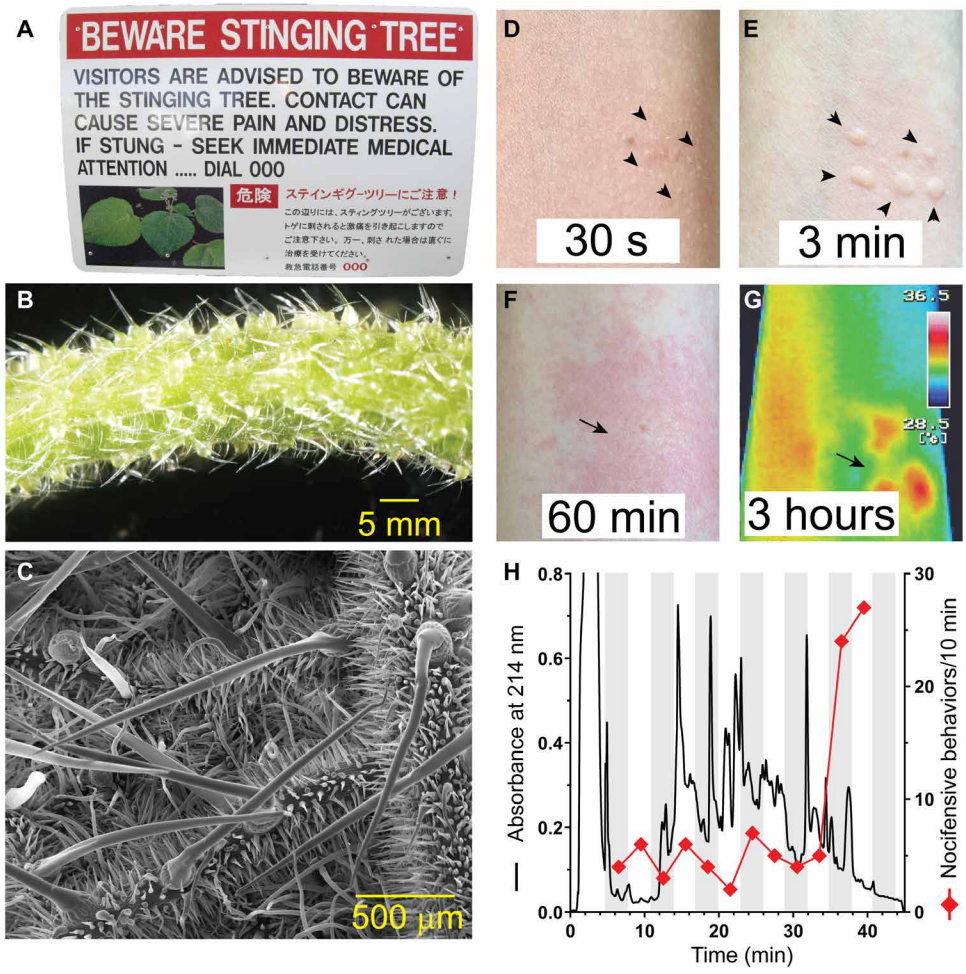

Fig. 1. Stinging nettles of the genus *Dendrocnide* produce potent neurotoxins. (**A**) Sign at a North Queensland National Park advising caution around stinging trees. (**B**) *D. excelsa* petioles are covered in stinging hairs. (**C**) Scanning electron micrograph of trichome structure on the leaf of *D. moroides*. (**D** to **G**) Cutaneous reaction resulting from an accidental sting with *D. moroides* documented with an iPhone XR and NEC G120W2 thermal imager, illustrating almost immediate local piloerection [arrowheads in (D)], development of wheals where stinging hairs penetrate the skin [arrows in (E)], as well as a long-lasting axon reflex erythema [arrows in (F) and (G)] and associated local increase in skin temperature (°C). (**H**) HPLC chromatogram of trichome extract from *D. excelsa*. Diamonds indicate nocifensive responses elicited by intraplantar administration of individual fractions in vivo in C57BL6/J mice, with a single late-eluting peak identified as the main pain-causing fraction. Photo credits: (A and D to G): Irina Vetter, The University of Queensland; (B): Thomas Durek, The University of Queensland; (C): Darren Brown, The University of Queensland.

the tip that effects envenomation by breakage and leakage of trichome contents. Contact with the trichomes during an accidental sting of a healthy 41-year-old individual resulted in an almost immediate sharp stinging sensation that was accompanied by local piloerection, wheals, and a slowly developing axon reflex flare persisting for several hours (Fig. 1, D to G). These cutaneous reactions were accompanied by painful sensations of increasing intensity, including deep aching and burning pain that can radiate to the ipsilateral axilla, and that is frequently interspersed by intermittent sharp stabbing pains. In addition to pain, crawling or tingling sensations and other paraesthesiae are also common symptoms in the experience of the authors. Although painful, treatment of the sting was not required.

To better understand the molecular basis for the observed pharmacological effects, we prepared stinging hair extracts from *D. excelsa*, fractionated the compound mixture via high-performance liquid chromatography (HPLC), and assessed the sensory effects of the resulting fractions in an in vivo model. A single, late-eluting peak (Fig. 1H) evoked nocifensive behaviors and was further characterized by mass spectrometry (MS): Matrix-assisted laser desorption/ionization MS (MALDI-MS) revealed several molecules with a mass of ~4 kDa, and reduction and alkylation coupled with tryptic digests further confirmed the presence of miniproteins containing three disulfide bonds (fig. S2A).

A short sequence tag, obtained via tandem MS, was used to interrogate a transcriptome assembled from RNA sequencing data of *D. excelsa* (fig. S2B). Further transcriptome analysis of *D. moroides* and complementary DNA (cDNA) cloning revealed a family of disulfide-rich peptides of 36 amino acid residues (Fig. 2A). The mature peptide sequences do not show any similarity to known sequences, although their cysteine pattern is similar to inhibitory cystine knot (ICK) peptides found in albumin-derived plant peptides and conotoxin Gm9a (Fig. 2 and fig. S2C) (*12*). The name chosen for these molecules from *Dendrocnide* trichomes, "gympietides," is derived from the name in the Gubbi Gubbi language for the stinging

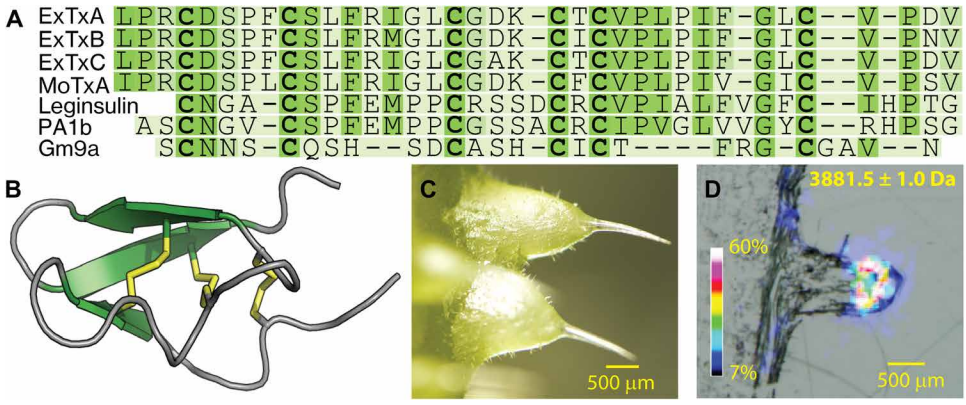

Fig. 2. Gympietides define a previously unidentified family of ICK peptides from stinging nettles. (**A**) Sequence alignment of 4-kDa miniproteins from *D. excelsa* (ExTxA-C) and *D. moroides* (MoTxA), as well as the structurally related ICK peptides leginsulin (*Glycine max*), PA1b (*Pisum sativum*), and conotoxin Gm9a (*Conus gloriamaris*). (**B**) NMR structure model of ExTxA. (**C**) Stinging trichomes of *D. excelsa* and (**D**) MALDI-IMS heat map distribution of *m/z* (mass/charge ratio) 3881.5 Da indicating trichome-specific expression of ExTxA. Photo credits (C and D): Thomas Durek, The University of Queensland.

trees (gympie-gympie) (*13*). To further delineate their nomenclature, peptides of this class from similar precursors are named with the prefix ExTx (Excelsatoxin, of *D. excelsa*) and MoTx (Moroidotoxin, of *D. moroides*). To unequivocally demonstrate the anticipated pharmacological activity of these molecules, we chemically synthesized ExTxA and MoTxA (fig. S3, A and B) and confirmed their structural identity with crude trichome extract–derived toxins via multiple reaction monitoring (MRM) MS (fig. S3C). Quantitative MRM analysis indicated a substantially higher abundance of ExTxA in trichome extracts compared to extracts prepared from the same aerial parts of the same plant but with the trichomes removed, further supporting a stinging hair–specific defense role of these molecules (fig. S4). Consistent with the putative neurotoxic action of the gympietides, sections of *D. excelsa* petioles examined with MALDI imaging revealed the presence of masses matching ExTxA (3881.5 Da; Fig. 2D) particularly in areas where stinging trichomes and trichome support cells are present.

The three-dimensional (3D) structure of synthetic ExTxA was determined by simulated annealing using nuclear magnetic resonance (NMR)–derived nuclear Overhauser effect (NOE) distance and angular restraints and deuterium exchange kinetics (fig. S5). The models confirm the anticipated ICK structure of ExTxA and, despite limited sequence similarity to other ICK peptides, further highlight the structural plasticity of this widespread peptide scaffold (Fig. 2B and fig. S5E).

Gympietide pharmacology

When injected into the hind paw of mice at low doses (0.1 to 1.2 pmol/40 µl), synthetic ExTxA and MoTxA faithfully and dose-dependently recapitulated the neurotoxic effects of *Dendrocnide* stings, causing nocifensive behavior (licking or biting and shaking or lifting of the affected paw) lasting for approximately 1 hour [nocifensive behaviors/1 hour: saline, 13 ± 4 (n = 3); ExTxA 1 nM, 8 ± 2 (n = 4); ExTxA 3 nM, 100 ± 17 (n = 6); ExTxA 10 nM, 173 ± 18 (n = 5); ExTxA 30 nM, 258 ± 30 (n = 6); MoTxA 10 nM, 421 ± 18 (n = 5)]. This behavior was accompanied by an axon reflex flare that was sustained for several hours after injection (ipsilateral paw temperature, 1 hour: 32.5 ± 0.3°C; contralateral paw temperature, 1 hour: 25.2 ± 0.2°C; $F_{6,28}$ = 17.25, P < 0.0001), resembling the reaction seen in humans (Figs. 1, F and G, and 3, A and B). We next assessed the effect of ExTxA on sensory nerve excitability using the murine skin–saphenous nerve preparation. Application of ExTxA (100 nM) to the receptive fields of mechanosensitive A- and C-fibers caused spontaneous action potential (AP) firing in most of the fibers, often inducing long-lasting high-frequency bursts (C-fiber APs/5 min: buffer, 0.8 ± 0.8; ExTxA, 191 ± 31; P = 0.0313; A-fiber APs/5 min: buffer, 0 ± 0; ExTxA, 251 ± 93, P = 0.0197) (Fig. 3, C to E), confirming direct activation of primary sensory neurons.

To gain insight into the pharmacological activity of ExTxA, we next assessed responses of dorsal root ganglion (DRG) neurons to ExTxA and MoTxA using fluorescence Ca^{2+} microscopy (Fig. 3, F to J, and fig. S6). Consistent with its neurotoxic effects, ExTxA caused Ca^{2+} influx in neurons, but not nonexcitable cells (fig. S6), with 68% of neurons (n = 523) (MoTxA; 73 ± 5%, n = 288) responding at a concentration of 10 nM ($\Delta F/F$ 2.080 ± 0.056) (Fig. 3, G to J, and fig. S6).

The excitatory effects of ExTxA were apparent in neurons of all sizes, including capsaicin-responsive nociceptors, and the proportion of neurons responding was significantly (F = 49.91, P = 0.0008) reduced to 26% (n = 146) in the presence of tetrodotoxin (TTX; 1 µM), suggesting activity at voltage-gated Na^+ channels (Fig. 3, G to J). We therefore assessed the effect of ExTxA (50 nM) on total voltage-gated Na^+ current using patch-clamp electrophysiology in DRG neurons and observed a notable delay in fast inactivation that resulted in a sustained current (I_{40ms}/I_{peak}: control, 0.04 ± 0.02; ExTxA, 0.31 ± 0.04; df = 7, P < 0.0001; Fig. 4, A and B). This sustained current was abolished by replacement of external Na^+ ions with choline and was inhibited by TTX (1 µM), confirming that ExTxA directly acts at voltage-gated sodium (Na_V) channels (Fig. 4C). In more detailed mechanism of action studies, we tested the gympietides using TE671 cells endogenously expressing the neuronal $Na_V1.7$, as confirmed by CRISPR knockdown experiments demonstrating significant decrease in current size (fig. S6, A and B). In $Na_V1.7$-expressing TE671 cells, ExTxA (1 µM) caused a significant hyperpolarizing shift in the voltage dependence of activation (Δ −7.2 mV, df = 4, P = 0.0014), with no significant effect on the voltage dependence of steady-state fast inactivation (Fig. 4D). Similarly, MoTxA (10 nM) shifted the voltage dependence of activation (Δ −7.2 mV, df = 6, P = 0.036) but not the voltage dependence of steady-state fast

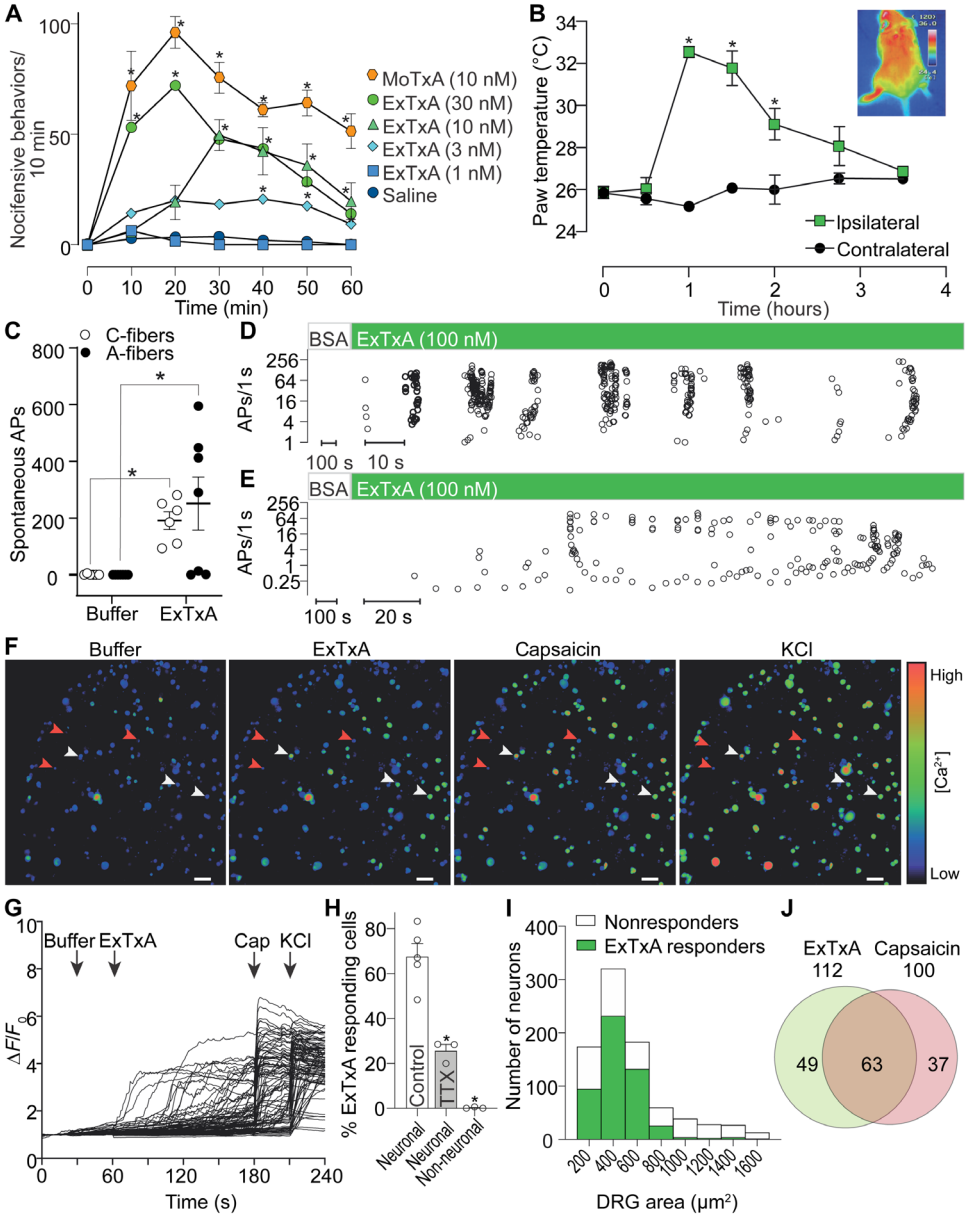

Fig. 3. Synthetic ExTxA and MoTxA activate sensory neurons in vivo and in vitro. (**A**) Intraplantar injection of synthetic ExTxA and MoTxA caused dose-dependent nocifensive behaviors in C57BL/6 mice as well as (**B**) local hyperemia resulting in a significant increase in skin temperature. Inset: Thermal image illustrating the ExTxA-induced axon reflex vasodilation. *$P < 0.05$ by repeated-measures two-way ANOVA; $n = 3$ to 6. (**C**) Exposure of the cutaneous receptive fields of sensory neurons to synthetic ExTxA caused spontaneous AP firing in A-fibers (black circles) and C-fibers (open circles). (**D** and **E**) Representative recordings from the murine skin–saphenous nerve preparation illustrating ExTxA-induced activity in A-fibers (D) and C-fibers (E). Open circles, APs plotted as instantaneous frequency. (**F** to **H**) ExTxA (10 nM) induces Ca^{2+} influx in DRG neurons (white arrows), including capsaicin-sensitive nociceptors, but not nonexcitable cells (red arrowheads). (F) Pseudocolor image illustrating Ca^{2+} responses in DRG neurons (scale bar, 100 μm), and (G) corresponding traces from all neurons of one representative experiment. (H) Total percentage of neuronal cells (±1 μM TTX) and non-neuronal cells responding to ExTxA (10 nM). (**I**) Distribution of ExTxA-responding and nonresponding DRG neurons by cell size and (**J**) overlap with capsaicin-sensitive nociceptors. Data are presented as means ± SEM; *$P < 0.05$.

inactivation, and lower concentrations of ExTxA (100 nM) also elicited qualitatively similar shifts in the voltage dependence of activation (Δ −5.6 mV, df = 6, $P = 0.013$) but not the voltage dependence of steady-state fast inactivation (fig. S6). Both ExTxA and MoTxA potently delayed Na_V inactivation in a concentration-dependent manner, with median effective concentrations (EC_{50}s) of 58 and 4 nM (pEC_{50} ExTxA, 7.24 ± 0.12; pEC_{50} MoTxA, 8.39 ± 0.18), respectively (Fig. 4E). Despite structural similarity to the gympietides, the most closely related pea-derived peptide PA1b (1 μM) had no effect on voltage-gated sodium currents (Fig. 4E). The effects of ExTxA on Na^+ currents were irreversible, with no apparent reduction in activity even after repeated wash steps over 30 min (Fig. 4F). Consistent with these pharmacological effects on Na_V channels, both TTX as well as the $Na_V1.7$-selective inhibitor Pn3a (*14*, *15*)

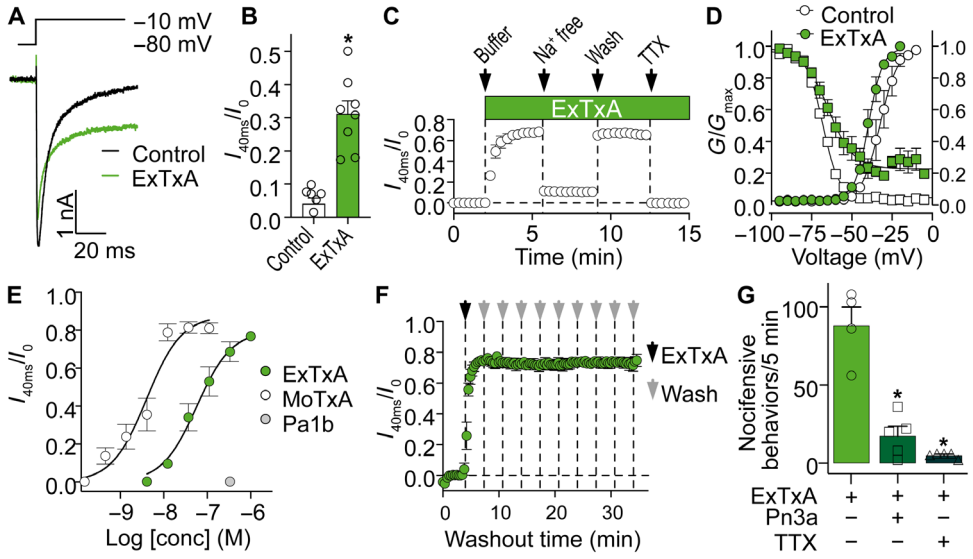

Fig. 4. ExTxA delays fast inactivation of voltage-gated sodium channels in sensory neurons. (**A** and **B**) ExTxA (50 nM) delays fast inactivation of voltage-gated Na^+ current in DRG neurons. (A) Representative Na^+ current trace and (B) total sustained current (40 ms from peak current), normalized to peak, from DRG neurons ($n = 8$). (**C**) Effect of ExTxA on sustained current is reversed by removal of external Na^+ and addition of TTX (1 μM) ($n = 5$). (**D**) Effect of ExTxA (green symbols) on the conductance-voltage (GV) curve of Na^+ current compared to control (white symbols). Circles, channel activation; squares, steady-state inactivation ($n = 3$). (**E**) Concentration-dependent effects of ExTxA, MoTxA, and PA1b on Na^+ current inactivation ($n = 4$ to 7 cells). (**F**) Effect of ExTxA (1 μM) on sustained current is not reversible with repeated wash steps. Black arrow, peptide addition; gray arrows, washout steps ($n = 4$; 35 min). (**G**) Co-administration of TTX (1 μM) or the $Na_V1.7$-selective inhibitor Pn3a (1 μM) with ExTxA by the intraplantar route significantly decreases in vivo nocifensive responses. $n = 5$ per group. Data are presented as means ± SEM; *$P < 0.05$.

decreased in vivo nocifensive behaviors elicited by ExTxA (Fig. 4G), suggesting that populations of neurons activated by ExTxA almost certainly include classical nociceptors defined by expression of $Na_V1.7$.

DISCUSSION

The intense pain sensations and prolonged axon reflex flare observed after envenomation by *Dendrocnide* species are consistent with the potent activity of the gympietides at Na_V channels, leading to activation of cutaneous neurons and neurotransmitter-mediated local vasodilation (*16*). Notably, although doses of the gympietides delivered by stinging hairs are difficult to estimate, our quantification of ExTxA content using MS places the approximate amount present in trichomes (2.5 to 5.0 pmol per trichome) close to doses eliciting symptoms of synthetic material in vivo (0.1 to 1.2 pmol per animal; Fig. 3, A and B). The comparatively smaller bicyclic peptide moroidin, which has been isolated from the leaves of *D. moroides* as well as *Celosia argentea* previously (*17*), consists of eight amino acid residues and has been thought to contribute to painful symptoms. However, moroidin, which is present at approximately 0.002% (w/w) in crude *D. moroides* leaf extract, only elicited a modest pain reaction after local injection of 10 μg of purified material, despite 1 μg of crude leaf extract eliciting a severe response (*18*, *19*). Our initial attempts to isolate moroidin to pharmacologically characterize the effects of this octapeptide on cultured sensory neurons failed, and we were unable to detect any of this compound in the trichomes or leaves of *D. excelsa*.

The extended duration of the nociceptive responses to *Dendrocnide* stings was replicated by injection of synthetic ExTxA in vivo and can be explained by the irreversible action of ExTxA on Na_V channels (Fig. 4), providing a pharmacological basis for the unique properties of the Australian stinging trees. This activity is particularly remarkable given that the primary structure of the gympietides is unique, with very limited similarity to known sequences. In contrast, the tertiary structure and function of these peptides are reminiscent of δ-therapotoxins, δ-hexatoxins, and δ-conotoxins from arachnid and cone snail venoms, respectively (fig. S5E). Hence, gympietides are the first plant-derived knottins with activity at Na_V channels reported to date, thus making them prototypic representatives of this previously unknown class of plant peptides. Their structural similarity and a delivery mode identifiable as envenomation exemplify cross-kingdom convergence of venoms (*20*). While the Australian stinging trees have evolved an effective defense against humans, and other mammals based on anecdotal reports, it remains unclear currently whether this defensive activity has contributed to the evolution of the gympietides or whether there are species differences in the pharmacological activity of this peptide class that may confer other benefits to these plants.

Although detailed structure-activity relationships remain to be explored, MoTxA was more potent than ExTxA, providing a possible explanation for anecdotal reports that stings from *D. moroides* are more severe than those from *D. excelsa* (*21*). While we cannot currently exclude activity at other neuronal targets, including other Na_V subtypes, modulation of $Na_V1.7$ by the gympietides sufficiently explains the observed in vitro and in vivo effects and suggests that Na_V channel blockers may provide pain relief to stinging tree victims clinically. The gympietides affected both channel inactivation and $V_{1/2}$ of activation, both of which may contribute to enhanced neuronal excitability. Notably, at higher ExTxA concentrations, there was also an increase in the fraction of noninactivated channels, despite the $V_{1/2}$ of inactivation being unaffected by both ExTxA and MoTxA at all concentrations tested.

Altering the activation threshold, combined with effects upon inactivation, likely leads to nociceptor activation and the sensation of pain, akin to biophysical changes observed in painful conditions associated with $Na_V1.7$ gain-of-function mutations such as inherited erythromelalgia (IEM) and paroxysmal extreme pain disorder (PEPD), respectively (*14*). As the gympietides bear little similarity to any other known Na_V modulators and display unusual effects particularly on Na_V inactivation, it is difficult to predict possible binding sites at this point. However, based on activity of animal venom–derived toxins and the biophysics of Na_V gating, the extracellular loops of the domain IV voltage sensor could be a possible binding site.

In summary, we show here that the active pain-causing principle in the stinging hairs of Australasian stinging trees *D. excelsa* and *D. moroides* is a family of ultrastable miniproteins that activate nociceptors by modulating inactivation of voltage-gated sodium channels expressed on sensory neurons. The 3D structure of these gympietides is reminiscent of animal venom toxins targeting the same receptors, thus representing a remarkable case of inter-kingdom convergent evolution of animal and plant "venoms." Our work clarifies the molecular basis for the pain caused by these plants while enabling structure-activity and convergent evolution studies to define how ancestrally distinct peptides in venoms may elicit the same response at pain receptors.

MATERIALS AND METHODS

Plant material

D. excelsa was collected near Mount Lindesay in southeast Queensland close to the New South Wales border (28°20.194′S, 152°40.403′E). *D. moroides* was collected near Atherton, far-north Queensland (17°10.608′S, 145°39.610′E and 17°19.889′S, 145°30.025′E). All plants were situated in disturbed nature strips alongside roads. Seeds of *D. moroides* were collected and sown in Jiffy peat pots and maintained at 28°C 16-hour/8-hour light/dark cycles under cool white fluorescent tubes. Upon attaining a size that could no longer be accommodated in the laboratory, seedlings were maintained at a mean temperature of 28°C in glasshouse conditions in a peat/sand soil and regular fertilization with a balanced fertilizer preparation.

Sample preparation for proteomics

Trichomes were isolated from expanding leaves still undergoing development by freezing petioles in liquid nitrogen and shaving off the trichomes with a scalpel. This procedure yields the silicified stinging hair attached to its multicellular base. Trichomes from several plants were combined, suspended in 50% acetonitrile (ACN)/H_2O, 0.1% trifluoroacetic acid (TFA) (~20 to 50 mg of trichomes/ml), and processed in a bead mill (SPEX SamplePrep, Metuchen, NJ, USA; Geno/Grinder, 2 × 2 min at 1200 rpm). The extract was cleared by centrifugation (10,000*g*, 5 min), and the supernatant was removed and lyophilized. Fractionation of the extract was achieved by dissolving 15 mg of lyophilized crude trichome extract in 50% ACN/H_2O, 0.1% TFA and separating the mixture on a C18 Luna RP HPLC column (10 × 250 mm) with a linear gradient of 10 to 80% B (90% ACN/H_2O, 0.08% TFA) in buffer A (0.1% TFA) over 35 min. Fractions were collected across the entire elution range and lyophilized.

Peptide synthesis

Gympietides were chemically synthesized by automated Fmoc SPPS using optimized protocols. Details for chemical synthesis parameters are available in the Supplementary Materials.

NMR spectroscopy and structure calculations

NMR spectroscopy was performed on Bruker Avance III 600 MHz or Neo 900 MHz spectrometers equipped with cryogenically cooled probes. Samples of synthetic ExTxA (2.4 mg) were dissolved in 500 µl of 40% (v/v) deuterated acetonitrile (ACN-D_3) in water. 2D total correlation spectroscopy (TOCSY) (80 ms mixing time), NOE spectroscopy (NOESY) (200 ms mixing time), exclusive correlation spectroscopy (E-COSY), and natural abundance heteronuclear correlation spectroscopy (^{15}N and ^{13}C-HSQC) were used to sequentially assign backbone and side-chain protons and heteroatoms. Variable temperature experiments were performed by recording six TOCSY spectra at temperatures ranging from 283 to 308 K. Slowly exchanging amide protons were identified by incubating ExTxA in 40% (v/v) ACN-D3 in D_2O over 24 hours. Solvent suppression was achieved using excitation sculpting. Spectra were referenced to water at 4.77 parts per million (ppm). All spectra were processed using TopSpin v3.6 and assigned using CcpNmr Analysis.

Distance restraints derived from the 900-MHz NOESY spectrum were used to calculate preliminary structures of ExTxA in CYANA, along with dihedral angles generated predicted by TALOS-N (*22*). Hydrogen bond pairs were added on the basis of these preliminary structures, amide proton temperature dependence, and slow deuterium exchange of proton donors. A final ensemble of structures was generated within central nervous system (*23*) using torsion angle dynamics and refinement and energy minimization in explicit water solvent. Stereochemical quality was assessed using MolProbity (*24*). Statistics describing the structural analyses are summarized in table S2.

Mass spectrometry

Details for sample preparation, tandem MS, targeted ultra-performance liquid chromatography (UPLC)–MS-MRM for quantification of neuromodulators, and MALDI imaging MS (MALDI-IMS) can be found in the Supplementary Materials.

Scanning electron microscopy

Plant samples for scanning electron microscopy were cut into small pieces and fixed in 2.5% glutaraldehyde in 0.1 M cacodylate buffer for 2 days and then postfixed in 1% osmium tetroxide for 1 hour, dehydrated through ethanol, and finally dried using the Tousimis Autosamdri Critical Point Dryer. Samples were mounted onto aluminum scanning electron microscopy stubs and coated with gold for 90 s. Images were captured using a JEOL JCM-5000 Neoscope scanning electron microscope (Laboratory Scientific Engineering) at 15 kV.

RNA sequencing and transcriptome analysis

RNA was extracted from flash-frozen young shoots of *D. excelsa* and *D. moroides* using TRIzol reagent according to the manufacturer's instructions. RNA sequencing was performed at the Australian Genome Research Facility (AGRF; Melbourne, Australia) on either an Illumina HiSeq 2500 platform (*D. excelsa*) or a NextSeq 6000 platform (*D. moroides*), all as paired-end runs. Data were deposited in the National Center for Biotechnology Information (NCBI) Short Read Archive under BioProject accession number PRJNA592832. Analysis pipeline and parameters are available in the Supplementary Materials.

Cloning of cDNA

Total RNA was reverse-transcribed into cDNA using SuperScript III reverse transcriptase (Invitrogen, Carlsbad, CA, USA) using the

oligo(dT) priming method provided by the manufacturer. Specific coding sequences of interest were amplified by high-fidelity polymerase chain reaction (PCR) using Phusion polymerase and primers designed at the start and stop of putative transcripts obtained in the assembled transcriptomes. Further details of primers used for cDNA cloning are available in the Supplementary Materials. Amplified products were purified from agarose gels and cloned into the vector pDS221 in BP Clonase (Invitrogen) reactions as per the manufacturer's protocol before the purified plasmids were Sanger-sequenced at the AGRF. The cDNA and coding sequences for these toxins were deposited in NCBI GenBank as MN784116 (ExTxA), MN784117(ExTxB), and MN784118 (MoTxA).

Animals

Adult male and female C57BL/6J mice aged 4 to 8 weeks were sourced from the Animal Resource Centre (Canning Vale, Western Australia). Animals were housed in groups of three or four per cage under 12-hour light-dark cycles and had standard rodent chow and water ad libitum. Ethical approval for experiments involving animals was obtained from The University of Queensland animal ethics committee. All experiments were conducted in accordance with the *International Association for the Study of Pain Guidelines for the Use of Animals in Research* and the *Australian Code of Practice for the Care and Use of Animals for Scientific Purposes*, 8th edition (2013).

Behavioral assessment and in vivo effects

ExTxA (1 to 30 nM) or MoTxA (10 nM) was diluted in saline/0.1% bovine serum albumin (BSA) and administered by intraplantar injection to the left hind paw of male mice in a volume of 40 µl under isoflurane (3%) anesthesia, and spontaneous pain behaviors (licks, bites, shakes, and lifts of the hind paw) were counted by a blinded investigator for 60 min after injection. To assess the effect of Na_V inhibitors, TTX (2 µM) or Pn3a (1 µM) was co-administered by intraplantar injection with ExTxA (30 nM), and spontaneous pain behaviors were counted 10 min after injection. In addition, the surface temperature of the hind paw skin was measured following intraplantar injection of ExTxA (30 nM) using a NEC G120W2 thermal camera at the time points stated. Images of cutaneous reactions after an accidental sting of an author, a 41-year-old healthy female with unremarkable medical history, with *D. moroides* were taken using an iPhone XR with iOS13.1.3 and a NEC G120W2 thermal camera at the time points stated. For statistical comparison of behavioral responses after intraplantar injection of ExTxA or buffer in C57BL/6 mice, a two-way analysis of variance (ANOVA) with time as a covariate using Sidak multiple comparisons test was used.

Single-fiber recordings

The saphenous nerve along with the skin of the dorsal hind paw and lower leg was removed from 6- to 8-week-old male and female C57BL/6J mice as previously described (*25*). The skin was placed in an organ chamber perfused with carbogenated synthetic interstitial fluid containing the following: 107.8 mM NaCl, 3.5 mM KCl, 0.69 mM $MgSO_4$, 26.2 mM $NaHCO_3$, 1.67 mM NaH_2PO_4, 9.64 mM Na-gluconate, 5.55 mM glucose, 7.6 mM sucrose, and 1.53 mM $CaCl_2$ (pH 7.3). The proximal end of the saphenous nerve was placed in a separate recording chamber immersed in paraffin oil and was desheathed and teased apart until a single fiber recording could be obtained. The receptive field was identified by mechanical probing and isolated using a plastic ring. We recorded from both high- and low-threshold mechanically excitable A- and C-fibers, which were distinguished based on conduction velocity and AP shape. Unfortunately, due to the size of the preparation and overlapping conduction velocity distributions, Aβ fibers can be difficult to distinguish from Aδ fibers in the murine skin–nerve preparation. We therefore included all A-fiber types in our analysis with the exception of rapidly adapting fibers that are myelinated touch fibers (*25*). Notably, we did observe activation of rapidly adapting Aβ fibers by ExTxA, consistent with nonselective activation of peripheral afferents particularly at high concentrations. Spontaneous APs were recorded 5 min before and 5 min after addition of ExTxA (100 nM). Data were recorded and analyzed using DAPSYS version 8. For statistical comparison of ExTxA-evoked AP firing, a two-tailed paired *t* test was used.

Cell culture

For Ca^{2+} imaging experiments, DRG neurons were isolated from 4- to 8-week-old male C57BL/6J mice as previously described (*26*, *27*). DRG neurons were dissociated and plated in 96-well poly-D-lysine–coated culture plates grown in Dulbecco's modified Eagle's medium supplemented with 10% fetal bovine serum (FBS) and penicillin/streptomycin. Isolated neurons were incubated for 24 hours at 37°C with 5% CO_2. For manual patch clamp experiments, DRG neurons were isolated from male and female C57BL/6J mice and placed in 2.5% collagenase type IV (Worthington, NJ, USA) for 3 hours (37°C, 5% CO_2). To further digest, ganglia were incubated with 2.5% trypsin (Sigma-Aldrich, MO, USA) for 15 min. Ganglia were triturated with flame-polished Pasteur pipettes and spun at 1000 rpm through a 15% (w/v) BSA gradient to remove myelin debris. Last, cells were plated on poly-D-lysine (PDL)/laminin-coated coverslips (Corning, NY, USA) with minimum essential medium (MEM) (Sigma-Aldrich) supplemented with 10% (v/v) FBS, 1% (v/v) penicillin/streptomycin, nerve growth factor (50 ng/ml) (Promega, WI, USA), and cytosine arabinoside (10 µM) and patched 16 to 24 hours after isolation.

TE671 cells endogenously expressing $Na_V1.7$ [ECACC (European Collection of Cell Cultures), Porton Down, Salisbury, United Kingdom] were cultured in MEM supplemented with 10% (v/v) FBS. Cells were grown in a humidified 5% CO_2 incubator at 37°C, grown to 70 to 80% confluence, and passaged every 3 to 4 days using TrypLE Express (Invitrogen).

SCN9A CRISPR knockout

Three custom pSpCas9(BB)-2A-Puro PX459 (GenScript, Nanjing, Jiangsu Province, China) encoding three separate guide RNAs (gRNAs) (gRNA_1: 5′-CCAGTCCGGTGGGTTATTCA-3′, gRNA_2: 5′-ACTTTCATAGTATTGAACAA-3′, gRNA_3: 5′-TATGACCATGAATAACCCAC-3′) that target SCN9A (gene encoding for Na_V 1.7) were generated. Plasmids were transfected into TE671 cells using Lipofectamine 3000 Transfection Reagent L30000015 (Life Technologies, Mulgrave, VIC, Australia) as per the manufacturer's protocol and selected by puromycin (1 µg/ml) (Life Technologies, Mulgrave, VIC, Australia). Na^+ currents in SCN9A knockdown and progenitor TE671 cells were tested using patch-clamp electrophysiology (fig. S6, A and B).

Calcium imaging

Dissociated DRG neurons were loaded with Fluo-4 AM calcium indicator (5 µM) for 1 hour in culture medium and then washed with assay solution (Hanks' balanced salt solution containing 20 mM

Hepes). Typically, 100 to 150 cells per well were used by examining fluorescence corresponding to $[Ca^{2+}]_i$ using a Nikon Ti-E Deconvolution inverted microscope, in conjunction with a Lumencor Spectra LED light source (excitation, 485 nm; emission, 521 nm). Images were acquired at 1 frame per second using a 20× objective. For each experiment, baseline fluorescence was observed for 20 s before addition of assay solution containing 0.1% BSA (negative control) at 30 s, 10 nM ExTxA or 10 nM MoTxA at 60 s, 1 μM capsaicin at 180 s, and 30 mM KCl (positive control) at 210 s. Excitable cells responding to KCl or capsaicin were classified as neuronal, while cells that did not respond to KCl were classified as non-neuronal (fig. S6C). Cells were classified as responders if they had at least a 1.5-fold increase in fluorescence over baseline. Any cells that responded to the negative control were excluded from analysis. For statistical comparison of ExTxA-induced Ca^{2+} responses in cultured DRG neurons, a one-way ANOVA using Tukey's multiple comparisons test was used.

Electrophysiology

Whole-cell patch clamp recordings were obtained at room temperature (20 ± 1°C) using an Axon MultiClamp 700B amplifier and pClamp (version 10) software (Molecular Devices, USA). Voltage-clamp intracellular solution (ICS) contained 130 mM CsF, 20 mM NaCl, 0.2 mM EGTA, 10 mM Hepes, 4 mM Mg–adenosine 5′-triphosphate, 0.3 mM Na–guanosine 5′-triphosphate, and 10 mM dextrose. Extracellular solution (ECS) contained 30 mM NaCl, 110 mM choline-Cl, 3 mM KCl, 1 mM $MgCl_2$, $CaCl_2$, 10 mM Hepes, 5 mM CsCl, 20 mM TEA (tetraethylammonium)–Cl, 0.1 mM $CdCl_2$, and 1 mM 4-aminopyridine (AP). ICS and ECS were adjusted to pH 7.2 with KOH or CsOH, and osmolarity was adjusted using glucose (300 to 310 mOsm and 310 to 320 mOsm, respectively). Pipettes were pulled from borosilicate glass (Warner, CT, USA) using Narishige PC-10 pipette puller on the day of experiment and fire-polished (Microforge MF-830, Narishige) to a resistance of 0.9 to 2 megohms. After whole-cell configuration was achieved, DRG neurons were held at −80 mV for voltage-clamp experiments. Low-sodium external solution was used to ensure that peak current size was kept well below 5 nA, ensuring adequate voltage control; therefore, voltage error was kept below ±5 mV using >70% series resistance compensation. Recordings were acquired at 20 kHz and filtered with a low-pass Bessel filter at 2.9 kHz. ExTxA (50 nM, 0.1% BSA) or ECS (0.1% BSA) was perfused onto neurons using gravity perfusion (5 ml/min), and pulses to −10 mV for 100 ms were used to quantify persistent current (average current amplitude during final 10 ms). For statistical comparison of Na^+ current in DRG neurons, a two-tailed paired *t* test was used.

Whole-cell patch-clamp experiments in TE671a cells endogenously expressing $Na_V1.7$ were performed on a QPatch-16 automated electrophysiology platform (Sophion Bioscience, Ballerup, Denmark) as previously described (*28*). The ECS contained 145 mM NaCl, 4 mM KCl, 2 mM $CaCl_2$, 1 mM $MgCl_2$, 10 mM Hepes, and 10 mM glucose (pH 7.4) (osmolarity, 305 mOsm). The ICS contained 140 mM CsF, 1 mM/5 mM EGTA/CsOH, 10 mM Hepes, and 10 mM NaCl (pH 7.3) with CsOH (osmolarity, 320 mOsm). *I-V* curves were obtained with a holding potential of −90 mV followed by a series of 500-ms step pulses that ranged from −110 to +55 mV in 5-mV increments (repetition interval, 5 s) before and after 5-min incubation with ExTxA (100 nM, 1 μM) or MoTxA (10 nM). Conductance-voltage curves were obtained by calculating the conductance (G) at each voltage (V) using the equation $G = I/(V - V_{rev})$, where V_{rev} is the reversal potential and was fitted with a Boltzmann equation. Voltage dependence of steady-state fast inactivation was tested using a 10-ms pulse of −20 mV immediately after the 500-ms step above to assess the available noninactivated channels. For statistical comparison on GV and steady-state inactivation curves, a two-tailed paired *t* test was used.

Concentration-response curves were acquired using a holding potential of −90 mV and a 50-ms pulse to −20 mV every 20 s (0.05 Hz). ExTxA, MoTxA, and PA1b were diluted in ECS with 0.1% BSA. Each peptide concentration was incubated for 5 min, and sustained current (40 ms from peak current) was normalized to peak current. For determination of the off-rate, ExTxA (1 μM) was incubated for 200 s before stepwise washout with ECS every 200 s for 30 min. Currents were elicited using a holding potential of −90 mV and a 50-ms pulse to −20 mV every 20 s (0.05 Hz).

Data analysis

Data were plotted and analyzed using GraphPad Prism version 8.2.0. Concentration-response curves were fitted to a four-parameter Hill equation with variable Hill coefficient. Statistical significance was defined as $P < 0.05$ using tests as indicated. Data are presented as means ± SEM.

SUPPLEMENTARY MATERIALS

Supplementary material for this article is available at http://advances.sciencemag.org/cgi/content/full/6/38/eabb8828/DC1

View/request a protocol for this paper from *Bio-protocol*.

REFERENCES AND NOTES

1. W. F. MacFarlane, The stinging properties of *Laportea*. *Econ. Bot.* **17**, 303–311 (1963).
2. P. A. Robertson, W. V. Macfarlane, Pain-producing substances from the stinging bush *Laportea moroides*. *Aust. J. Exp. Biol. Med. Sci.* **35**, 381–394 (1957).
3. D. Maor, M. Little, Skin contact with a stinging tree requiring intensive care unit admission. *Contact Dermatitis* **77**, 335–337 (2017).
4. C. Schmitt, P. Parola, L. de Haro, Painful sting after exposure to dendrocnide sp: Two case reports. *Wild. Environ. Med.* **24**, 471–473 (2013).
5. A. Mustafa, H.-J. Ensikat, M. Weigend, Stinging hair morphology and wall biomineralization across five plant families: Conserved morphology versus divergent cell wall composition. *Am. J. Bot.* **105**, 1109–1122 (2018).
6. A. J. Cummings, M. Olsen, Mechanism of action of stinging nettles. *Wild. Environ. Med.* **22**, 136–139 (2011).
7. H. Schildknecht, Irritant and defense substances of higher plants—A chemical herbarium. *Angew. Chem. Int. Ed.* **20**, 164–184 (1981).
8. N. Emmelin, W. Feldberg, The mechanism of the sting of the common nettle *Urtica urens*). *J. Physiol.* **106**, 440–455 (1947).
9. H. O. J. Collier, G. B. Chesher, Identification of 5-hydroxytryptamine in the sting of the nettle (*Urtica dioica*). *Brit. J. Pharmacol. Chemother.* **11**, 186–189 (1956).
10. F. Oliver, E. U. Amon, A. Breathnach, D. M. Francis, P. Sarathchandra, A. K. Black, M. W. Greaves, Contact urticaria due to the common stinging nettle (*Urtica dioica*)—Histological, ultrastructural and pharmacological studies. *Clin. Exp. Dermatol.* **16**, 1–7 (1991).
11. H. Y. Fu, S. J. Chen, R. F. Chen, W. H. Ding, L. L. Kuo-Huang, R. N. Huang, Identification of oxalic acid and tartaric acid as major persistent pain-inducing toxins in the stinging hairs of the nettle, *Urtica thunbergiana*. *Ann. Bot.* **98**, 57–65 (2006).
12. L. A. Miles, C. Y. Dy, J. Nielsen, K. J. Barnham, M. G. Hinds, B. M. Olivera, G. Bulaj, R. S. Norton, Structure of novel P-superfamily spasmodic conotoxin reveals an inhibitory cystine knot motif. *J. Biol. Chem.* **277**, 43033–43040 (2002).
13. J. Bell, A. Seed, *Dictionary of the Gubbi-Gubbi and Butchulla Languages* (J. Bell, 1994), 166 pp.
14. I. Vetter, J. R. Deuis, A. Mueller, M. R. Israel, H. Starobova, A. Zhang, L. D. Rash, M. Mobli, $Na_V1.7$ as a pain target—From gene to pharmacology. *Pharmacol. Ther.* **172**, 73–100 (2017).
15. J. R. Deuis, Z. Dekan, J. S. Wingerd, J. J. Smith, N. R. Munasinghe, R. F. Bhola, W. L. Imlach, V. Herzig, D. A. Armstrong, K. J. Rosengren, F. Bosmans, S. G. Waxman, S. D. Dib-Hajj, P. Escoubas, M. S. Minett, M. J. Christie, G. F. King, P. F. Alewood, R. J. Lewis, J. N. Wood, I. Vetter, Pharmacological characterisation of the highly $Na_v1.7$ selective spider venom peptide Pn3a. *Sci. Rep.* **7**, 40883 (2017).

16. K. Zimmermann, J. R. Deuis, M. C. Inserra, L. S. Collins, B. Namer, P. J. Cabot, P. W. Reeh, R. J. Lewis, I. Vetter, Analgesic treatment of ciguatoxin-induced cold allodynia. *Pain* **154**, 1999–2006 (2013).
17. H. Morita, K. Shimbo, H. Shigemori, J. Kobayashi, Antimitotic activity of moroidin, a bicyclic peptide from the seeds of *Celosia argentea*. *Bioorg. Med. Chem. Lett.* **10**, 469–471 (2000).
18. P. B. Oelrichs, P. A. Robertson, Purification of pain-producing substances from dendrocnide (*Laportea*) moroides. *Toxicon* **8**, 89–90 (1970).
19. T.-W. C. Leung, D. H. Williams, J. C. J. Barna, S. Foti, P. B. Oelrichs, Structural studies on the peptide moroidin from *Laportea moroides*. *Tetrahedron* **42**, 3333–3348 (1986).
20. D. R. Nelsen, Z. Nisani, A. M. Cooper, G. A. Fox, E. C. K. Gren, A. G. Corbit, W. K. Hayes, Poisons, toxungens, and venoms: Redefining and classifying toxic biological secretions and the organisms that employ them. *Biol. Rev.* **89**, 450–465 (2014).
21. M. Hurley, in *Beating Around the Bush* (The Conversation, 2018); https://theconversation.com/the-worst-kind-of-pain-you-can-imagine-what-its-like-to-be-stung-by-a-stinging-tree-103220.
22. Y. Shen, A. Bax, Protein backbone and sidechain torsion angles predicted from NMR chemical shifts using artificial neural networks. *J. Biomol. NMR* **56**, 227–241 (2013).
23. A. T. Brünger, P. D. Adams, G. M. Clore, W. L. DeLano, P. Gros, R. W. Grosse-Kunstleve, J.-S. Jiang, J. Kuszewski, M. Nilges, N. S. Pannu, R. J. Read, L. M. Rice, T. Simonson, G. L. Warren, Crystallography & NMR system: A new software suite for macromolecular structure determination. *Acta Crystallogr. D* **54**, 905–921 (1998).
24. V. B. Chen, W. B. Arendall III, J. J. Headd, D. A. Keedy, R. M. Immormino, G. J. Kapral, L. W. Murray, J. S. Richardson, D. C. Richardson, MolProbity: All-atom structure validation for macromolecular crystallography. *Acta Crystallogr. D* **66**, 12–21 (2010).
25. K. Zimmermann, A. Hein, U. Hager, J. S. Kaczmarek, B. P. Turnquist, D. E. Clapham, P. W. Reeh, Phenotyping sensory nerve endings in vitro in the mouse. *Nat. Protoc.* **4**, 174–196 (2009).
26. T. R. Cummins, A. M. Rush, M. Estacion, S. D. Dib-Hajj, S. G. Waxman, Voltage-clamp and current-clamp recordings from mammalian DRG neurons. *Nat. Protoc.* **4**, 1103–1112 (2009).
27. S. D. Robinson, A. Mueller, D. Clayton, H. Starobova, B. R. Hamilton, R. J. Payne, I. Vetter, G. F. King, E. A. B. Undheim, A comprehensive portrait of the venom of the giant red bull ant, *Myrmecia gulosa*, reveals a hyperdiverse hymenopteran toxin gene family. *Sci. Adv.* **4**, eaau4640 (2018).
28. M. C. Inserra, M. R. Israel, A. Caldwell, J. Castro, J. R. Deuis, A. M. Harrington, A. Keramidas, S. Garcia-Caraballo, J. Maddern, A. Erickson, L. Grundy, G. Y. Rychkov, K. Zimmermann, R. J. Lewis, S. M. Brierley, I. Vetter, Multiple sodium channel isoforms mediate the pathological effects of pacific ciguatoxin-1. *Sci. Rep.* **7**, 42810 (2017).
29. A. M. Bolger, M. Lohse, B. Usadel, Trimmomatic: A flexible trimmer for illumina sequence data. *Bioinformatics* **30**, 2114–2120 (2014).
30. M. G. Grabherr, B. J. Haas, M. Yassour, J. Z. Levin, D. A. Thompson, I. Amit, X. Adiconis, L. Fan, R. Raychowdhury, Q. Zeng, Z. Chen, E. Mauceli, N. Hacohen, A. Gnirke, N. Rhind, F. di Palma, B. W. Birren, C. Nusbaum, K. Lindblad-Toh, N. Friedman, A. Regev, Full-length transcriptome assembly from RNA-seq data without a reference genome. *Nat. Biotechnol.* **29**, 644–652 (2011).
31. P. Song, O. S. Mabrouk, N. D. Hershey, R. T. Kennedy, In vivo neurochemical monitoring using benzoyl chloride derivatization and liquid chromatography-mass spectrometry. *Anal. Chem.* **84**, 412–419 (2012).

Acknowledgments: We acknowledge the facilities and the scientific and technical assistance of Microscopy Australia and the Centre for Microscopy and Microanalysis, The University of Queensland. **Funding:** This work was funded by Australian Research Council (ARC) discovery projects [DP150100443 (E.K.G., D.J.C., and T.D.), DP200102377 (I.V. and T.D.), ARC Laureate fellowship (FL150100146 (D.J.C.)]; NHMRC fellowships APP1162503 (I.V.), APP1139961 (J.R.D.), and APP1176209 (J.L.S.); and Medical Research Council MR/S003428/1.
Author contributions: I.V. and T.D. conceived the project and designed experiments. S.J., J.R.D., M.R.I., S.D.R., D.A., and I.V. performed pharmacological analysis. E.K.G., F.B.H.R., and T.D. collected plant samples and performed RNA sequencing experiments, data analysis, and cDNA cloning. T.D. performed chemical synthesis, and P.J.H. and T.D. analyzed NMR data. D.J.C. oversaw structural studies and facilitated fieldwork. A.G.P. and B.R.H. performed MALDI-IMS experiments, and D.L.B. and J.L.S. acquired the scanning electron microscopy images. K.Y. and A.G.P. performed quantitative MS analysis and de novo peptide sequencing. E.K.G., S.J., J.R.D., I.V., and T.D. prepared the manuscript. All authors contributed to editing of the manuscript. **Competing interests:** The authors declare that they have no competing interests. **Data and materials availability:** RNA sequencing data were deposited in the NCBI Short Read Archive (SRA) under BioProject accession number PRJNA592832. Coding sequences of Gympietides were deposited in NCBI GenBank MN784116 (ExTxA), MN784117 (ExTxB), and MN784118 (MoTxA). The structure of ExTxA was deposited in RCSB Protein Data Bank (PDB ID: 6VH8) and chemical shift data in Biological Magnetic Resonance Data Bank (BMRB entry: 30711). All other data are available in the main text or the Supplementary Materials.

Submitted 24 March 2020
Accepted 2 July 2020
Published 16 September 2020
10.1126/sciadv.abb8828

Citation: E. K. Gilding, S. Jami, J. R. Deuis, M. R. Israel, P. J. Harvey, A. G. Poth, F. B. H. Rehm, J. L. Stow, S. D. Robinson, K. Yap, D. L. Brown, B. R. Hamilton, D. Andersson, D. J. Craik, I. Vetter, T. Durek, Neurotoxic peptides from the venom of the giant Australian stinging tree. *Sci. Adv.* **6**, eabb8828 (2020).